



Manage and Trail of AC/AC Sparse Modular Multilevel Converter

¹ PG Scholar, Dept of EEE(PE), KLR College of Engineering& Technology, Paloncha, Bhadradi Kothagudem, Telangana, India.
²Assistant Professor, Dept of EEE, KLR College of Engineering& Technology, Paloncha, Bhadradi Kothagudem, Telangana, India
³H.O.D., Dept of EEE, KLR College of Engineering& Technology, Paloncha, Bhadradi Kothagudem, Telangana, India

ABSTRACT

The sparse modular multilevel converter (MMC) is a new kind of high-voltage ac/ac MMC topology reasonable for high power applications. It depends on an elective setup of half/full-connect sub modules, and voltage UN folder organizes on each side of the converter. This topology has less parts thought about to traditional methodologies and as an extra advantage, the greater part of the switches work under the delicate exchanging condition. A thorough control system is proposed to guarantee capacitor voltage adjusting while at the same time misusing the full power ability of the converter. An altered un folder is additionally recommended to take out the inborn zero-intersection flowing current. The viability of the proposed control technique is gotten by recreation also, exploratory outcomes.

I. INTRODUCTION

WITH THE consistently expanding progression in semiconductor gadgets, high power voltage source converters (VSCs) have been pulling in more consideration in numerous modern applications, for example, sustainable power source asset interfaces, flexible ac transmission systems (FACTS) gadgets and HVDC lines [1]– [3]. In huge numbers of these applications, two AC systems with diverse frequencies are associated, or variable recurrence capacity is wanted. Fragmentary Frequency Transmission System (FFTS) is an illustration that utilizations low recurrence to lessen the line reactance, and to build its ability. FFTS has been utilized in

European railroad zap frameworks for very nearly a century [4], [5]. As of late, AC/AC converters were proposed to lessen the weight and misfortunes in footing impetus frameworks [6]– [8]. Different illustrations are high voltage machine drives [9]– [11]. A consecutive (B2B) 2-level VSC is a notable topology that utilizes a DC-connection to associate two AC sources [12]. A few topologies are proposed to lessen its part tally, yet they confront constraints in the methods of activity and may require complex control frameworks [13]. For higher voltage levels, B2B staggered converters are typically utilized as they can give high voltage yield with to a great degree low bending and lower dv/dt , while the semiconductor gadgets just need to endure a bit

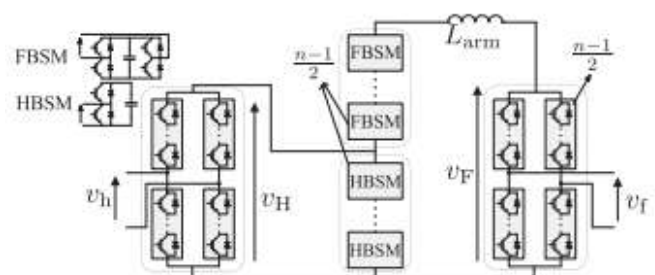


Fig. 1 Schematic diagram of a single-phase n-level SMMC

of the DC voltage. The intricacy of the capacitor voltage adjusting in diode-clipped converter (DCC) is unraveled in the B2B form, yet like flying capacitor converter (FCC) and fell H-bridge converters (HBC), it experiences high number of parts. Multilevel modular converter (MMC) is proposed in



2003 to beat such constraints by using low voltage switches and offering low consonant bending Presently, MMC-based HVDC frameworks are offered for control transmission up to GW ranges. Particular staggered lattice converter is first presented in 2001 and after that further got produced for engine drive applications. High number of hard-exchanged semiconductors and undesired coursing streams are the disadvantages of MMC and particular staggered lattice converter which are impressively enhanced in Sparse Modular Multilevel Converter (SMMC).

In this paper, a control procedure in view of third-consonant infusion is proposed for SMMC to ensure the capacitor voltage adjusting in various operational conditions. Furthermore, an altered UN folder is proposed to dispose of the characteristic zero-intersection flowing current. Whatever remains of the paper is sorted out as takes after. Initial, a concise depiction on taking out zero-intersection coursing current is talked about in Section II. Segment III presents the hypothetical examination of capacitor voltage adjusting. This is taken after by actualizing a control methodology in view of the hypothetical discoveries in Section IV. The usefulness of the proposed voltage adjusting control framework, is affirmed by both recreation also, test in Section V and VI, separately. At last, Segment VII exhibits the conclusions.

II. CHANGED SPARSE MODULAR MULTILEVEL CONVERTER

Fig. 1 demonstrates the schematic outline of a solitary stage sparse modular Multilevel Converter (SMMC). The SMMC comprises of two low recurrence UN folders on the sides and one leg

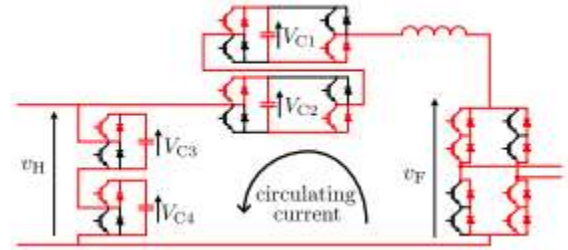


Fig. 2 Zero-crossing circulating current in a 5-level SMMC

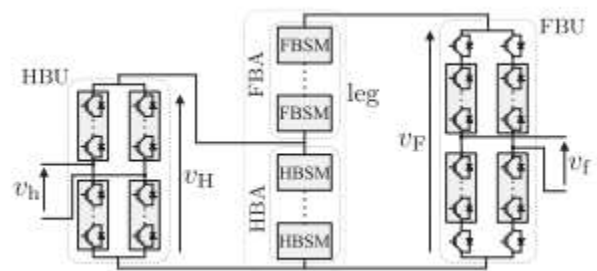


Fig. 3 Schematic diagram of a modified single-phase SMMC

Containing various cascade full bridges (FBSM) and half bridge sub modules (HBSM) by embeddings appropriate number of SMs in the upper and lower arms, the coveted voltage on both sides of the converter can be accomplished. Not at all like MMC, there is no flowing current between various legs (stages) of SMMC, as they are disengaged from each other by a 3-stage transformer. Be that as it may, it is naturally feasible for current to flow inside one period of the SMMC. This current isn't nonstop and may just stream when v_F crosses zero, thus it is called zero-intersection flowing current. For instance, in Fig. 2, if $VC_3 + VC_4$ is somewhat littler than $VC_1 + VC_2$, it makes v_F turn into a little negative esteem (when $v_F = 0$ is required). Likewise, due to exchanging homeless people, the SM inclusion/bypassing may not happen at the same time. This prompts one additional level decline/increment in v_F for a brief timeframe. An additional level abatement in v_F (at the point when $v_F = 0$ is required),



could make v_F negative. This negative voltage turns on the unfolder's hostile to parallel diodes and current courses through the leg. The arm inductor is introduced to constrain this current.

Two main considerations in deciding the cost of arm inductor are its inductance and its ostensible current. This inductor is on the way of the whole exchanged power; accordingly it must have the capacity to consistently withstand the aggregate current without immersion which makes it a major detached segment nearly as practically identical to the AC-channel inductor. Including one turned around IGBT in each arm of the FB-side Unfolded (FBU) could square the conceivable little negative v_F as appeared in Fig. 3 and deters the need of the arm inductor. The HB-side unfolder (HBU) stays flawless. It ought to be seen that the most extreme voltage-drop over the turned around IGBT happens, when half-bridge arm (HBA) and full-bridge arm (FBA) capacitors are in their most minimal and most elevated adequate voltages, separately. In this way, this IGBT must withstand the predefined capacitor voltage swell, ΔV_{ripp} duplicated by the quantity of HBSMs (or FBSMs) which equivalents to $(n - 1)/2 \times \Delta V_{ripp}$. This suggests on the off chance that

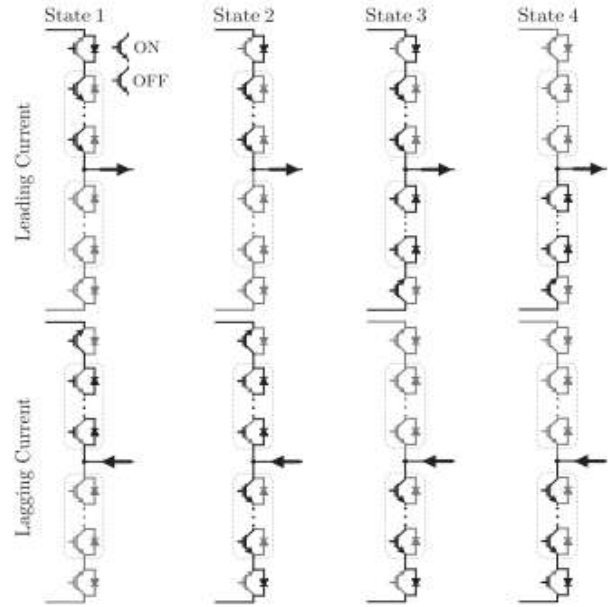


Fig. 4 Description of zero-crossing transition in FBU

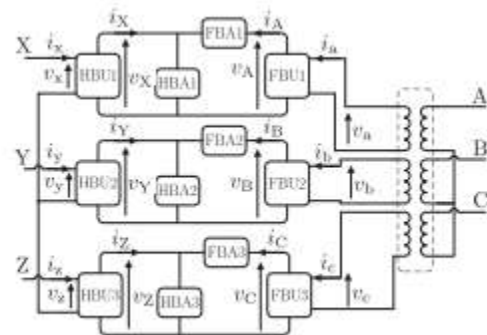


Fig. 5 Schematic diagram of a 3-phase SMMC

of high number of levels, in excess of one turned around IGBT may be required. The extra IGBT is a piece of the unfolder arm which is a series of arrangement associated semiconductor gadgets. This requires both transient and relentless state voltage sharing among the gadgets. The unfolders work in zero-voltage switching (ZVS) mode, along these lines transient voltage sharing is constantly fulfilled.

In the off-state, relentless state voltage sharing is accomplished by introducing high-esteem parallel resistors.



The extra IGBT must be furnished with a similar resistor. Fig. 4 shows FBU's rule of task at voltage zero-intersection progress for both driving and slacking streams. It can be seen that at any phase of progress, there is no less than one turned around IGBT obstructing the zero crossing circling current. The 3-stage SMMC is built utilizing a 3-stage transformer as appeared in Fig. 5.

III. CAPACITOR VOLTAGE BALANCING

Fig. 6 demonstrates the disentangled schematic graph of a single phase SMMC. The voltages and streams on the FB-and

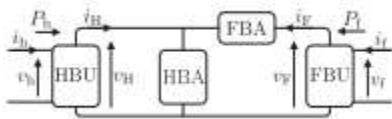


Fig. 6 Streamlined schematic outline of a solitary stage SMMC

HB-sides of the converter can be spoken to as:

$$v_f = V_m f \sin(\omega f t), v_F = \lambda_f \cdot v_f, \lambda_f = \text{sign}(v_f)$$

$$i_f = I_m f \sin(\omega f t - \phi_f), i_F = \lambda_f \cdot i_f \tag{1}$$

$$v_h = V_m h \sin(\omega h t + \theta_h), v_H = \lambda_h \cdot v_h, \lambda_h = \text{sign}(v_h)$$

$$i_h = I_m h \sin(\omega h t + \theta_h - \phi_h), i_H = \lambda_h \cdot i_h \tag{2}$$

As indicated by Fig. 6, the momentary power experiencing FBA and HBA are ascertained as:

$$p_{HB}(t) = (i_F + i_H) \times v_H, p_{FB}(t) = i_F \times (v_F - v_H). \tag{3}$$

In the consistent state condition, the put away vitality of FBA and HBA must be steady, so the capacitor voltages stay unaltered. This prompts the accompanying conditions:

$$\int_T p_{HB}(t) \cdot dt = 0, \int_T p_{FB}(t) \cdot dt = 0.$$

Eq. (4) is rewritten as following criteria:

$$\int_T (p_{FB}(t) + p_{HB}(t)) \cdot dt = 0, \int_T p_{FB}(t) \cdot dt = 0.$$

The first criterion leads to the real power balance between the AC-sides as presented below:

$$0 = \int_T (p_{FB}(t) + p_{HB}(t)) \cdot dt$$

$$= \int_T (i_F \times v_F + i_H \times v_H) \cdot dt$$

$$= \frac{1}{2} V_{mf} I_{mf} \cos(\varphi_f) + \frac{1}{2} V_{mh} I_{mh} \cos(\varphi_h)$$

$$\Rightarrow P_f + P_h = 0.$$

The second criterion is studied as:

$$0 = \int_T p_{FB}(t) \cdot dt = \int_T \{i_F \times (v_F - v_H)\} \cdot dt$$

$$\Rightarrow \frac{1}{2} V_{mf} I_{mf} \cos(\varphi_f) = \int_T (i_F \times v_H) \cdot dt$$

$$= V_{mh} I_{mf} \int_T \{\lambda_f \sin(\omega_f t - \varphi_f) |\sin(\omega_h t + \theta_h)|\} \cdot dt.$$

This can be rewritten as:

$$\frac{V_{mf}}{V_{mh}} = \int_T \frac{2\lambda_f \sin(\omega_f t - \varphi_f) |\sin(\omega_h t + \theta_h)|}{\cos(\varphi_f)} \cdot dt$$

$$= \int_T g(t) \cdot dt - \int_T h(t) \cdot dt,$$

$$g(t) = 2 |\sin(\omega_f t) \sin(\omega_h t + \theta_h)|,$$

$$h(t) = 2\lambda_f \cos(\omega_f t) \tan(\varphi_f) |\sin(\omega_h t + \theta_h)|.$$

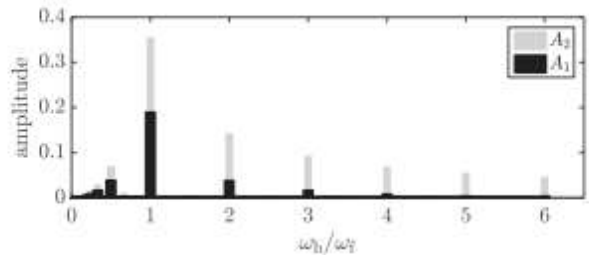


Fig. 7 The estimation of A1 and A2 in light of ω_h/ω_f



There is no diagnostic answer for Eq. (8). Be that as it may, its numerical arrangement can be approximated as:

$$G = \int_T g(t) \approx 0.81 + A_1 \cos(B.\theta_h),$$

$$H = \int_T h(t) \approx A_2 \tan(\varphi_f) \sin(B.\theta_h).$$

A. The effect of recurrence proportion

Accept the AC-side frequencies are not a whole number various of each other ($\omega_h/\omega_f = m$ or $1/m$ where m is a whole number). For this situation, as it is appeared in Fig. 7, A_1 and A_2 are steady what more, relatively equivalent to 0 is. For example, if the converter works between two frameworks with the frequencies of 50 Hz and 60 Hz, $A_1 = 0.0001$ and $A_2 = 0.0028$. Expecting that v_f side isn't absolutely inductive, by substituting A_1 and A_2 in Eq. (11)

$$M \approx 0 \Rightarrow \frac{V_{mf}}{V_{mh}} \approx 0.81.$$

Hence, the AC-side voltage proportion measures up to 0.81 paying little mind to the recurrence proportion. As indicated by Eq. (11), regardless of whether the recurrence proportion is a little whole number, the voltage proportion would even now be steady, yet it could be influenced by AC-sides control factor and stage point. At the end of the day, if voltage adjusting is accomplished, the converter's pick up is dependably a settled esteem. In the following area, third symphonious infusion is proposed to control the converter's increase, paying little respect to the recurrence proportion.

B. Voltage Ratio Regulation

For some pragmatic applications, voltage proportion control is fundamental. For instance, in network associated application, voltage pick up can be utilized to modify the receptive power trade with the AC systems. The AC-side voltages can be controlled by infusing music, with the end goal that the proportion between the normal corrected Air

conditioning voltage and its central segment is balanced. In this process, the unfolders are wanted to hold the delicate exchanged activity. All in all, the two sides of the converter can contribute to the voltage proportion control by conceding an unbounded arrangement of music. In any case, the additional music ought to be picked such that they are counteracted in line-line voltages. At the end of the day, just odd products of three sound (3, 9, 15, 21... ∞) can be utilized. For instance, the voltage control is performed utilizing just third consonant expansion to transformer-side of the converter (see Fig. 5). In light of this procedure, the AC-side voltages in a 3-stage SMMC appeared in Fig. 5 can be spoken to as:

$$\begin{cases} v_a = V_{mf} \sin(\omega_f t) + V_3 \sin(3\omega_f t + \beta) \\ v_b = V_{mf} \sin(\omega_f t - 2\pi/3) + V_3 \sin(3\omega_f t + \beta) \\ v_c = V_{mf} \sin(\omega_f t - 4\pi/3) + V_3 \sin(3\omega_f t + \beta) \\ v_U = \lambda_u v_u, \lambda_u = \text{sign}(v_u), u = a, b, c \end{cases}$$

$$\begin{cases} v_x = V_{mh} \sin(\omega_h t + \theta_h) \\ v_y = V_{mh} \sin(\omega_h t + \theta_h - 2\pi/3) \\ v_z = V_{mh} \sin(\omega_h t + \theta_h - 4\pi/3) \\ v_U = \lambda_u v_u, \lambda_u = \text{sign}(v_u), u = x, y, z \end{cases}$$

Presently, it is wanted to create voltage adjusting conditions for one period of the SMMC (e.g. the stage amongst A_n and X). As indicated by Fig. 5, the immediate power experiencing $FBA1$ and $HBA1$ are:

$$p_{HB1}(t) = (i_A + i_X) \times v_X, p_{FB1}(t) = i_A \times (v_A - v_X).$$

The impartial terminal of the transformer isn't grounded, hence the additional third symphonious voltage does not make current and in this way can't add to the power stream. Therefore, like past segment, the primary foundation of voltage adjusting leads to the genuine power adjusts between the AC-sides. The second foundation of voltage adjusting eqs. Prompts:



$$VR = \frac{V_{mf}}{V_{mh}} = \int_T \frac{2\lambda_a \sin(\omega_f t - \varphi_f) |\sin(\omega_h t + \theta_h)|}{\cos(\varphi_f)} dt.$$

The effect of stage point θ_h and recurrence proportion are examined previously. Along these lines, for effortlessness, in this area, it is accepted that $\theta_h = 0$ and furthermore the recurrence proportion is anything but a little whole number.

IV. CONTROL STRATEGY

The proposed converter could be controlled in either abc frame where PR controller is utilized or in d-q-outline as appeared in Fig. 11. To control the AC-side streams in d-q frames, a synchronization component is accomplished through a phase Locked Loop (PLL) on each side of the converter with ability of info DC-blunder dismissal. Two reference generators are used to give the reference AC streams to the following control arrange. Pfref in Grid F decides the sum also, heading of exchanged genuine power, while the receptive forces, Qfref and Qhref are managed to discretionary qualities inside the rating of converter. On each side of the converter, a standard current controller is utilized as delineated in Fig. 12, which gives the normal dynamic and responsive power trade with the matrix.

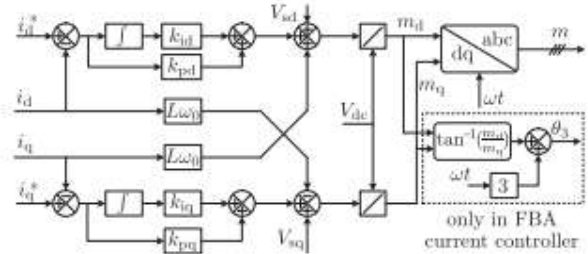


Fig. 12 The schematic outline of the present controller

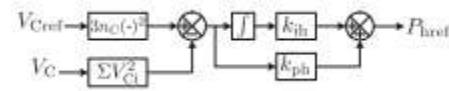


Fig. 13 The schematic outline of HBA Energy Balancing unit

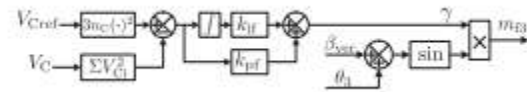


Fig. 14 The schematic outline of FBA Energy Balancing unit

In the event that the capacitor voltages have a few motions, sounds can be rejected from the AC-side streams and voltages if a changed PWM is utilized. To direct the aggregate vitality put away in the capacitors, a moderate external control circle is utilized on each side of the converter. To do as such, the capacitor voltage reference (V_{Cref}) and its deliberate esteem are squared and increased by the aggregate number of SMs in the arm, which gives the coveted and estimated vitality put away in the arm.

By modifying the aggregate vitality put away in the arm capacitors, the harmony between the arm control and the AC-side dynamic power is kept up. For the HB-side, the interior control variable of P_{href} is given by the aggregate vitality put away in the HBAs as outlined in Fig. 13. n_C is the aggregate number of capacitors in each arm which is equivalent to $(n - 1)/2$ of every an n -level SMMC. For the FB-side, as specified in the past area, the power stream could be controlled by infusing third symphonious voltage. Fig. 14 shows the way toward giving γ which at that point is utilized

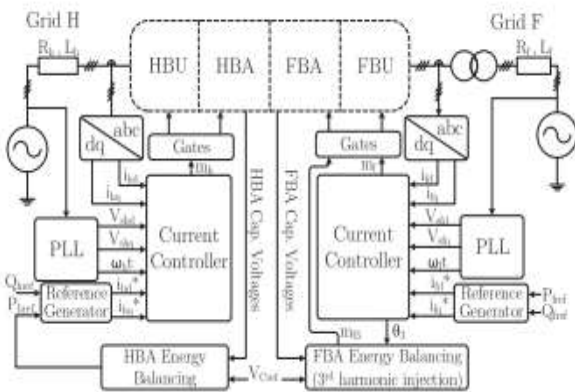


Fig. 11 The schematic outline of control procedure



to create the third consonant part. $\beta_{ver} (\approx 0.8 \pi$ or $-0.8 \pi)$ is the stage point that creates the most elevated/least voltage proportion. It is additionally important to equitably appropriate the arm vitality between the capacitors by choosing

TABLE I
SIMULATION PARAMETERS

Parameter	Rating
Power rating	S_{conv} 4 MVA
Grid H & F frequencies	f_b, f_f 60 Hz, 50 Hz
Grid H & F voltages (line-line rms)	V_{SH}, V_{SF} 9 kV, 7.3 kV
SM capacitor	C_{SM} 4 mF
Mean cell capacitor voltage	E 2000 V
Filter + Grid inductance	L_f, L_b 5 mH
Filter + Grid resistance	R_f, R_b 10 m Ω

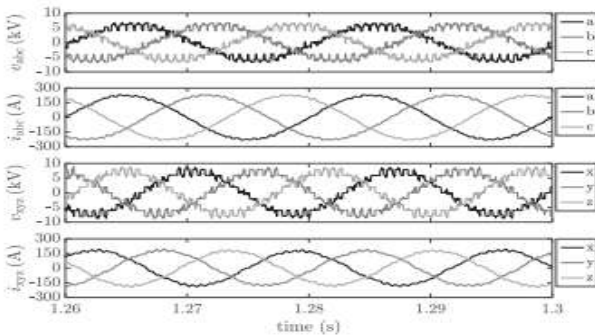


Fig. 15 Enduring state voltage and current waveforms

the best possible SMs at each time. This is finished by the arranged line of capacitor voltages and arm current bearing [22].

V. SIMULATION RESULTS

The hypothetical discoveries for a 3-stage SMMC appeared in Fig. 5 are approved by recreation utilizing MATLAB/Simulink programming. In this recreation, the HB-side of the converter is associated with Matrix H with

recurrence of 60 Hz, while the opposite side is associated to Grid F working at 50 Hz. The converter is evaluated for 4 MVA what's more, the capacitors' normal voltage are controlled at 2 kV. Table I records the principle reenactment parameters. A multi-bearer PWM is connected to the converter with the end goal that the compelling recurrence of the yield voltage is 1500 Hz. By having four SMs in each arm, the exchanging recurrence of SM IGBTs is around 375 Hz, while the unfold switches work at relating AC line recurrence. By and by, the quantity of levels is higher agreeing to the coveted power and AC-side voltages. Hence, the waveform quality would enhance and littler AC channels could be introduced.

Fig. 15 demonstrates the consistent state voltages and streams. The dynamic control streams from Grid F to Grid H, while the power factor for the two sides is solidarity. Along these lines, the FB-and HB-sides of the converter work as a rectifier and an inverter, separately. It can be seen that the third consonant part of the AC-side voltages is counterbalanced and the coveted major part is all around combined. It must be noticed that the voltages appeared in Fig. 15 are considered as interior parameters of the converter what's more, situated before the AC-side channels. As said in the past segment, on each side of the converter, a present controller

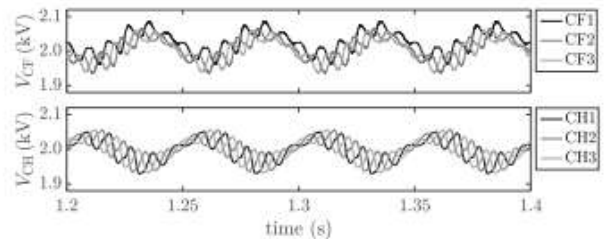


Fig. 16 Steady-state average HBA and FBA capacitor voltages

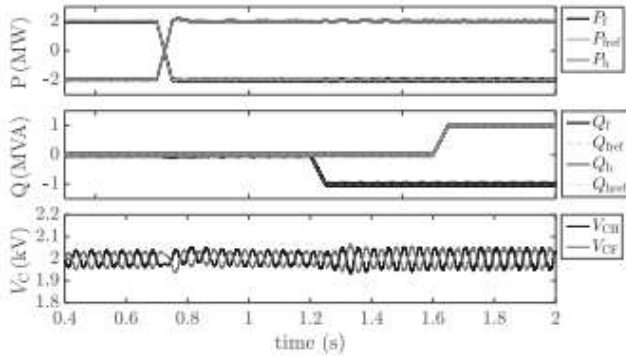


Fig. 17 Converter transient waveforms during power variation

is used to guarantee an AC sinusoidal current with adequate symphonious substance (see Fig. 12). The present controller is quick enough to moderate the effect of capacitor voltage swell on the current by changing the converter's AC-side voltage. Fig. 16 shows the conduct of the capacitor voltages in the relentless state condition. The top to-crest swell in the capacitor voltage is around 8% which may differ due to the working purpose of dynamic and responsive powers on the two sides of the converter. Since the infused third-consonant voltage does not make present, third-consonant recurrence does not show up in capacitor voltages.

The 20 Hz swell is caused by the converters characteristic vitality adjusting cycle. Note that the recurrence of the redressed AC-voltages (and thusly present) gets multiplied (i.e. 100 Hz and 120 Hz) and a short time later, the best normal factor of the amended streams' frequencies shows up as the regular recurrence of converter's vitality adjusting cycle (here, $GCD(100, 120) = 20$ Hz). To consider the dynamic reaction of the converter, a couple of dynamic and receptive power changes are connected on the two sides as rising/falling slope inside 5 ms. As appeared in Fig. 17, the coveted working point is appropriately controlled by its reference. Amid every transient, a little blunder may happen in

the capacitor voltages which will be repaid in a couple of cycles.

VI. EXPLORATORY RESULTS

Fig. 18 demonstrates a low-scale single-stage 5-level SMMC built utilizing MOSFET gadgets (MTD6N15T4G). The control framework is actualized on a dSPACE-Micro Lab Box unit. In this setup, the HB-side of the converter is associated with the network (120 V and 60 Hz), while the FB-side feeds a resistive stack working at 98 V and 50 Hz. The parameters of the exploratory setup can be found in Table II. Here, the exchanging

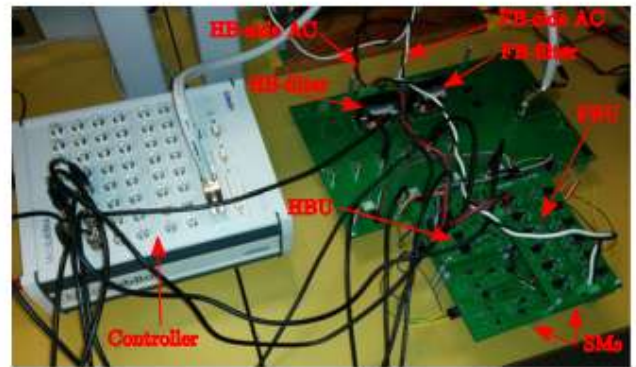


Fig. 18 A view of the experimental setup

TABLE II
EXPERIMENTAL PARAMETERS

Parameter		Rating
HB & FB sides' frequency	f_h, f_l	60 Hz, 50 Hz
HB & FB sides' AC voltage (rms)	$V_{ac,h}, V_{ac,l}$	120 V, 98 V
SM capacitor	C_{SM}	820 μ F
Mean cell capacitor voltage	E	100 V
MOSFET maximum drain-source voltage	V_{DS}	150 V
MOSFET continuous drain current	I_D	6 A
MOSFET drain-source on-state resistance	R_{DS-ON}	300 m Ω
Filter inductance	L_S, L_L	5 mH

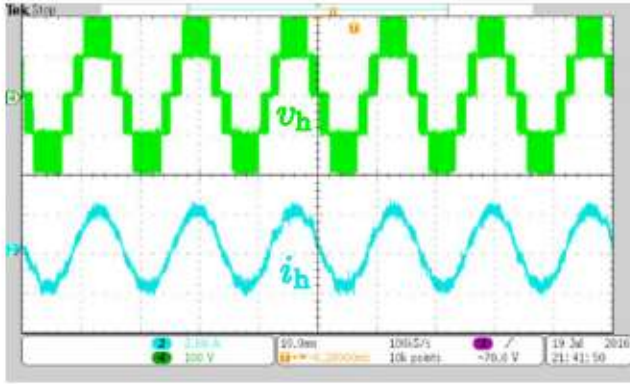


Fig. 19 Converter's HB-side waveforms in enduring state condition

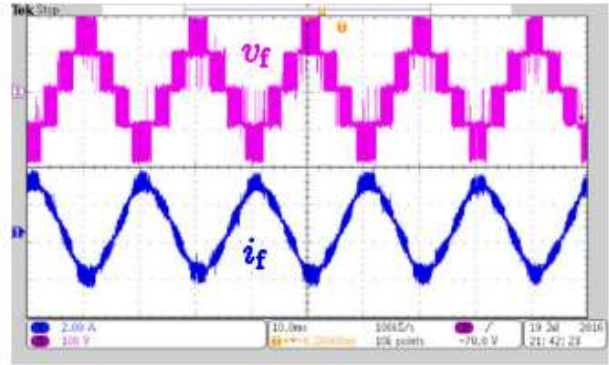


Fig. 20 Converter's FB-side waveforms in consistent state condition

Recurrence of 3 kHz is connected to the SM switches which could be diminished by using higher number of SMs. For a single phase SMMC without third-consonant infusion and with recurrence proportion of $60/50 = 1.2$, the voltage proportion is consistent and nearly levels with $V_m f/V_{mh} \approx 0.81$. The receptive power on both sides is set to zero. With exchanging just dynamic power, in request to accomplish control adjusts, the present proportion is required to be $I_m f/I_{mh} \approx 1.23$. The converter's HB-and FB-side consistent state waveforms are appeared in Figs. 19 and 20, separately. Both side streams are estimated as they enter the converter and the voltages are estimated before the AC-side channels (see Fig. 6). It can be seen that both side voltages are very much incorporated with the normal plentifulness and recurrence.

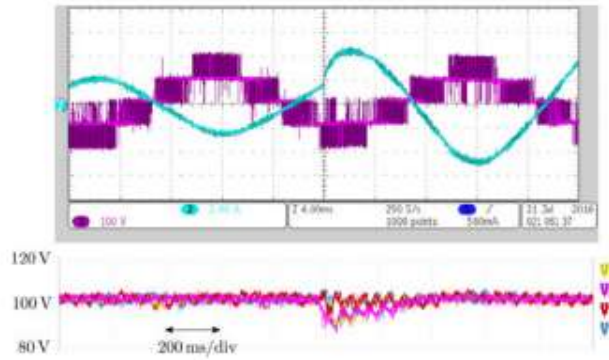
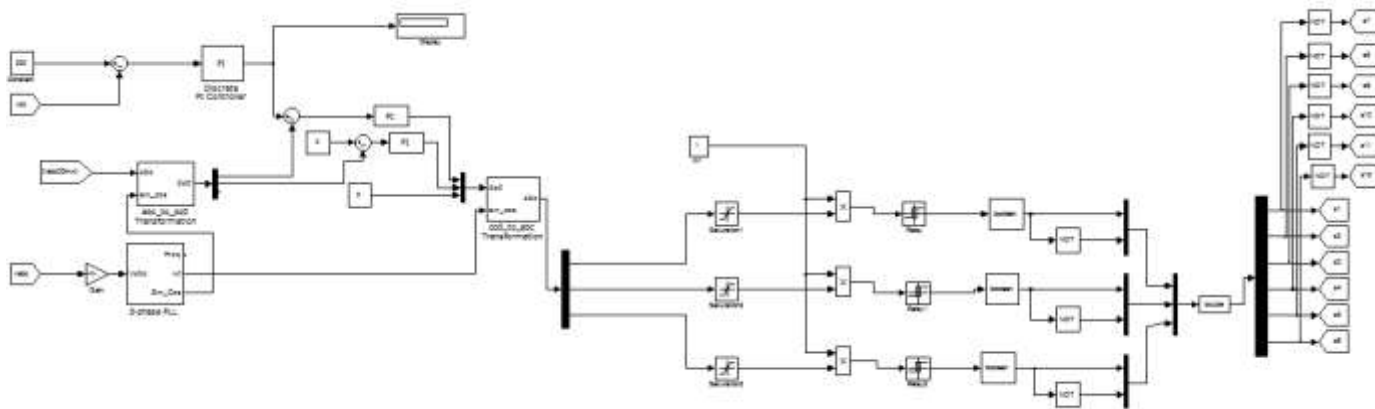
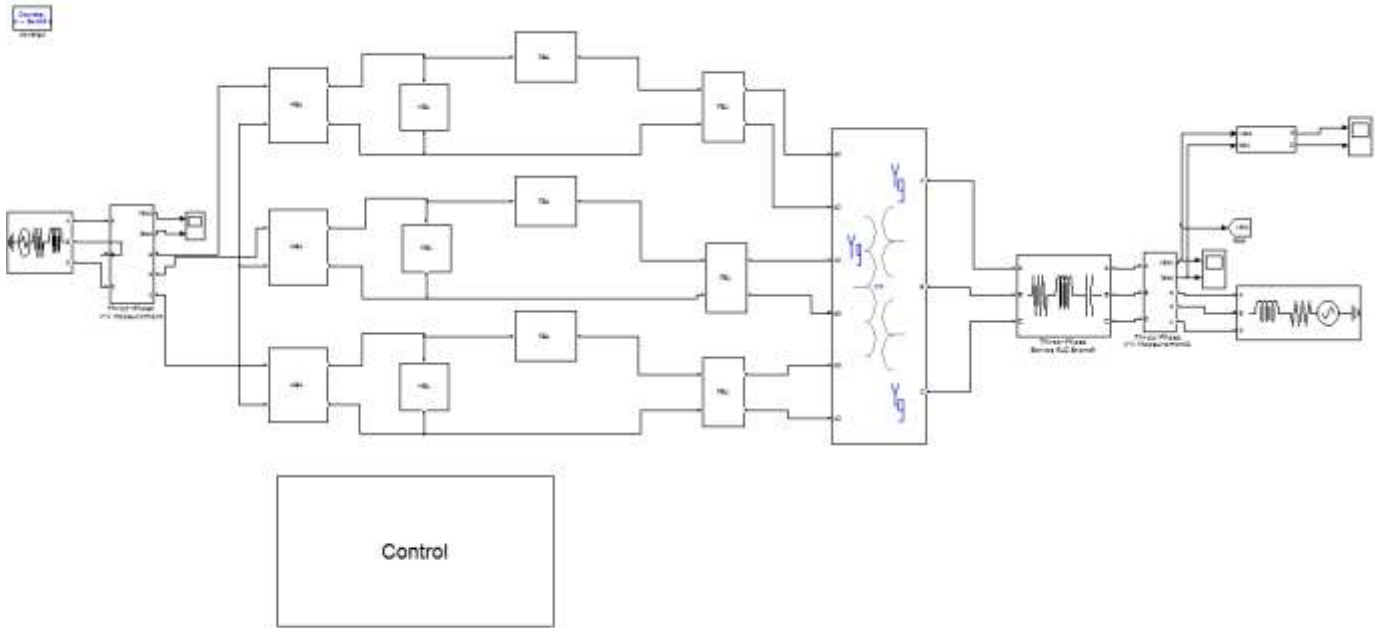


Fig. 21 Dynamic reaction of the converter to the heap change Keeping in mind the end goal to assess the dynamic reaction of the capacitor voltage adjusting system, the heap is abruptly multiplied while the SM capacitor voltages are observed. As appeared in Fig. 21, a sudden increment in the heap makes the capacitors lose a little segment of their put away vitality which would be recognized by both HBA and FBA vitality adjusting units (see Figs. 13 and 14). Subsequently, the activity point will be redesigned and the capacitors' vitality will be reestablished in less than 300 ms.

SIMULATION MODEL



SIMULATION RESULTS

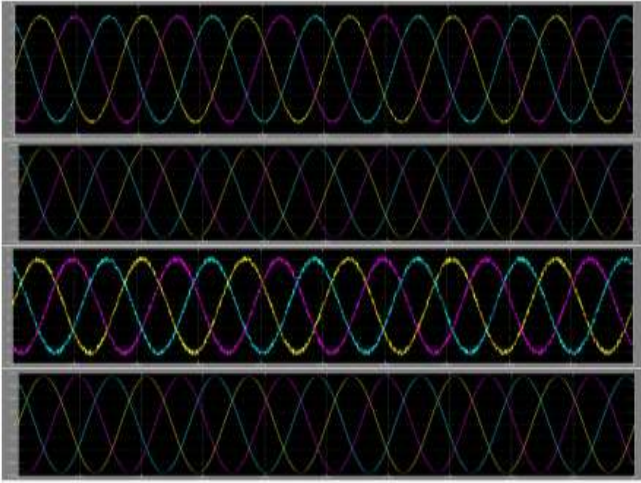


Fig. 1 Steady-state voltage and current waveforms

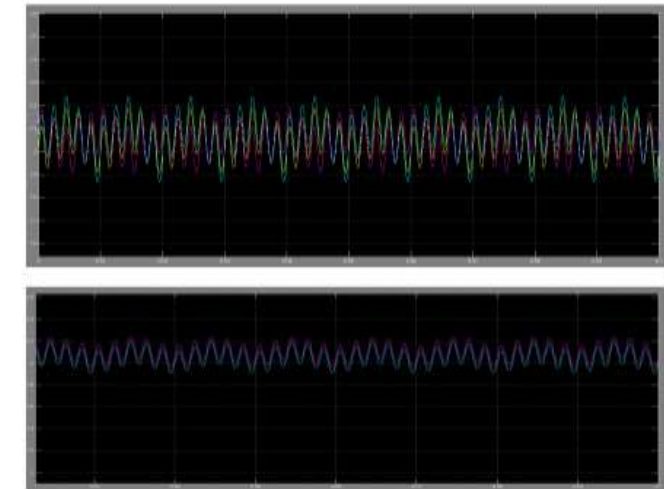
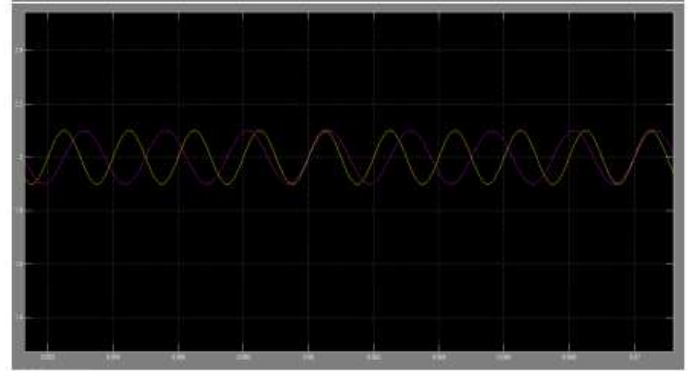
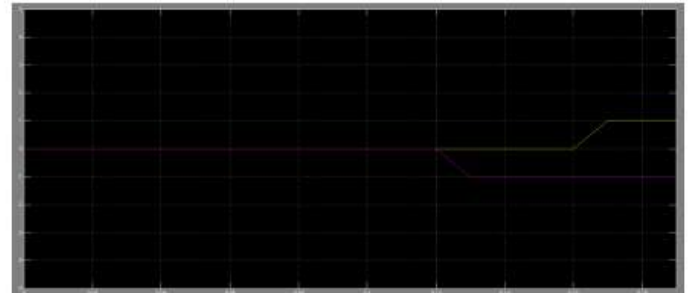
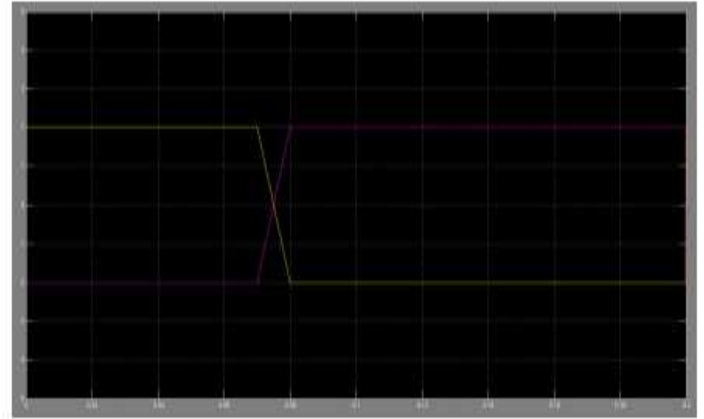


Fig. 2 Steady-state average HBA and FBA capacitor voltages

Fig.3 Converter transient waveforms during power variation

VII. CONCLUSION

The proposed control technique guarantees the capacitor voltage adjusting in various working frequencies by infusing third symphonious voltage segment which is significant to



completely abuse the capacities of a SMMC. Likewise, a change of SMMC is proposed to enhance the converter's execution. Both reenactments what's more, trial results demonstrate that SMMC can satisfy the prerequisites of a bidirectional AC/AC converter.

REFERENCES

- [1] A. Lotfjou, Y. Fu, and M. Shahidehpour, "Half breed AC/DC transmission development arranging," *IEEE Trans. Power Del.*, vol. 27, no. 3, pp. 1620–1628, Jul. 2012.
- [2] S. A. Khajehoddin, P. K. Jain, and A. Bakhshai, "Fell staggered converters and their applications in photovoltaic frameworks," in *Proc. second Can. Sol. Structures Conf.*, Calgary, AB, Canada, Jun. 2007, pp. 10–14.
- [3] M. Saeedifard and R. Iravani, "Dynamic execution of a particular staggered consecutive HVDC framework," *IEEE Trans. Power Del.*, vol. 25, no. 4, pp. 2903–2912, Oct. 2010.
- [4] X. Wang and X. Wang, "Practicality investigation of partial recurrence transmission framework," *IEEE Trans. Power Syst.*, vol. 11, no. 2, pp. 962–967, May 1996.
- [5] W. Xifan, C. Chengjun, and Z. Zhichao, "Investigation on partial recurrence transmission framework," *IEEE Trans. Power Syst.*, vol. 21, no. 1, pp. 372–377, Feb. 2006.
- [6] A. Rufer, N. Schibli, C. Chabert, and C. Zimmermann, "Configurable front-end converters for multi current trains worked on 16 2/3 Hz Air conditioning and 3 kV DC frameworks," *IEEE Trans. Power Electron.*, vol. 18, no. 5, pp. 1186–1193, Sep. 2003.
- [7] P. Drabek, Z. Peroutka, M. Pittermann, and M. Cedi, "New arrangement ' of footing converter with medium-recurrence transformer utilizing grid converters," *IEEE Trans. Ind. Electron.*, vol. 58, no. 11, pp. 5041–5048, Nov. 2011.
- [8] A. Gomez-Exposito, J. M. Mauricio, and J. M. Maza-Ortega, "VSC-based MVDC railroad zap framework," *IEEE Trans. Power Del.*, vol. 29, no. 1, pp. 422–431, Feb. 2014.
- [9] L. M. Tolbert, F. Z. Peng, and T. G. Habetler, "Staggered converters for expansive electric drives," *IEEE Trans. Ind. Appl.*, vol. 35, no. 1, pp. 36–44, Jan. 1999.
- [10] M. Kazerani, "An immediate AC/AC converter in view of current-source converter modules," *IEEE Trans. Power Electron.*, vol. 18, no. 5, pp. 1168–1175, Sep. 2003.
- [11] A. K. Jain and V. Ranganathan, "Cross breed LCI/VSI control circuit—A general high-control converter answer for wound field synchronous engine drives," *IEEE Trans. Ind. Electron.*, vol. 58, no. 9, pp. 4057–4068, Sep. 2011.
- [12] B. Wu, *High-Power Converters and AC Drives*. Hoboken, NJ, USA: Wiley, 2006.
- [13] G.-T. Kim and T. Lipo, "VSI-PWM rectifier/inverter framework with a diminished switch tally," *IEEE Trans. Ind. Appl.*, vol. 32, no. 6, pp. 1331–1337, Nov./Dec. 1996.
- [14] C. B. Jacobina, I. Soares de Freitas, and A. M. N. Lima, "DC-interface threephase-to-three-stage four-leg converters," *IEEE Trans. Ind. Electron.*, vol. 54, no. 4, pp. 1953–1961, Aug. 2007.

AUTHOR'S PROFILE

STUDENT PROFILE



D.MALLESHAM received B.Tech degree in Electrical and Electronics Engineering KBR College of Engineering, Pagidipalli, Yadadri Bhongir (Dist), Telengana, and currently pursuing M.Tech in Power Electronics & Electrical Drives at KLR College of Engineering & Technology,



Paloncha, Bhadradi Kothagudem (Dist) , TS. My areas of interest are Electrical Machines, Power Systems and Power Electronics.

GUIDE PROFILE

M.RAVINDAR Working as Assistant Professor in Electrical and Electronics Engineering at KLR College of Engineering & Technology, Paloncha, Bhadradi



Kothagudem, Telangana. He received the B.Tech Degree in Electrical and Electronics Engineering from Sarada Institute of Technology and Science, Rangunadhapalam, Ballepalli, Khammam, Telangana. He obtained his M.Tech degree in Power

Electronics from Pulipati Institute of Technology, Khammam, and Telangana. He has a Teaching Experience of 5 years. His interested areas were Power Electronics, Power Systems, Control systems, Electrical circuits and Electrical Machines.

H.O.D. PROFILE

V.NARESH KUMAR Working as a H.O.D and Assistant Professor in Electrical and Electronics Engineering at KLR College of Engineering & Technology, Paloncha, Bhadradi



Kothagudem, T.S, He received the B.Tech Degree in Electrical and Electronics Engineering from Adams Engineering College, Paloncha, JNTUH, T.S, and he received P.G. In Electrical

and Electronics Engineering as Electrical Power Systems is Specialization at Abdulkalam Institute of Technological Sciences, Bhadradi Kothagudem, T.S, He has a Teaching Experience of 8 years. His Areas of Interest are Power Systems, Control systems, Electrical Machines, Power Electronics and Static Drives.